Journal of Controlled Release 350 (2022) 600–612

Contents lists available at ScienceDirect

Journal of Controlled Release

journal homepage: www.elsevier.com/locate/jconrel

Surface analysis of sequential semi-solvent vapor impact (SAVI) for studying microstructural arrangements of poly (lactide-*co*-glycolide) microparticles

John Garner [a], Sarah Skidmore [a], Justin Hadar [a], Haesun Park [a], Kinam Park [a,b,*], Bin Qin [c], Yan Wang [c]

[a] Akina, Inc., West Lafayette, IN 47906, USA
[b] Purdue University, Biomedical Engineering and Pharmaceutics, West Lafayette, IN 47907, USA
[c] Food and Drug Administration, Center for Drug Evaluation and Research, Office of Generic Drugs, Office of Research and Standards, Silver Spring, MD 20993, USA

ARTICLE INFO

Chemical compounds:
2-Pentanone
Toluene
Butanone
Ethyl acetate
Lactide
Glycolide
Butyl acetate
Ethyl isobutyrate
Propyl acetate

Keywords:
PLGA
Laser scanning confocal microscopy
Semi-solvent vapor
Surface morphology
Long-acting injectable formulation

ABSTRACT

Biodegradable poly(lactide-*co*-glycolide) (PLGA) microparticles have been used as long-acting injectable (LAI) drug delivery systems for more than three decades. Despite extensive use, few tools have been available to examine and compare the three-dimensional (3D) structures of microparticles prepared using different compositions and processing parameters, all collectively affecting drug release kinetics. Surface analysis after sequential semi-solvent impact (SASSI) was conducted by exposing PLGA microparticles to different semi-solvent in the liquid phase. The use of semi-solvent liquids presented practical experimental difficulties, particularly in observing the same microparticles before and after exposure to semi-solvents. The difficulties were overcome by using a new sequential semi-solvent vapor (SSV) method to examine the morphological changes of the same microparticles. The SASSI method based on SSV is called surface analysis of semi-solvent vapor impact (SAVI).

Semi-solvents are the solvents that dissolve PLGA polymers depending on the polymer's lactide:glycolide (L:G) ratio. A sequence of semi-solvents was used to dissolve portions of PLGA microparticles in an L:G ratio-dependent manner, thus revealing different structures depending on how microparticles were prepared. Exposing PLGA microparticles to semi-solvents in the vapor phase demonstrated significant advantages over using semi-solvents in the liquid phase, such as in control of exposure conditions, access to imaging, decreasing the time for sequential exposure of semi-solvents, and using the same microparticles. The SSV approach for morphological analysis provides another tool to enhance our understanding of the microstructural arrangement of PLGA polymers. It will improve our comprehensive understanding of the factors controlling drug release from LAI formulations based on PLGA polymers.

1. Introduction

Poly(lactide-*co*-glycolide) (PLGA) microparticles have been used for more than three decades as long-acting injectable (LAI) depot systems to deliver various drugs for up to six months. More than a dozen PLGA microparticle formulations have been approved by the U.S. Food and Drug Administration (FDA). Despite the extensive use of PLGA polymers, their physicochemical properties have not been characterized in detail until recently [1–7]. One unique property of PLGA polymers is that their dissolution in various solvents depends on the lactide:glycolide (L:G) ratio. To date, all PLGAs used in drug delivery have L:G ratios ≥50:50, e.g., 65:35, 75:25, and 85:15. Some solvents dissolve PLGAs with all L:G ratios, e.g., dioxane, chloroform, dichloromethane, dimethyl sulfoxide, and dimethylformamide. Many solvents, however, have limited ability to dissolve PLGAs depending on the L:G ratio. Thus, they are named "semi-solvents" due to this conditional solubilizing property. These semi-solvents have been recently categorized and ranked based on their capacity to dissolve, under standardized conditions, at least 10 mg/mL of an 80 kDa PLGA ($L_{10mg/mL}$) at a specific L:G ratio [1,2,4–6]. Due to their partial solubility for PLGA, semi-solvents have been used to identify individual PLGAs from a mixture of PLGAs having different L:G ratios and molecular weights [4].

* Corresponding author at: Akina, Inc., West Lafayette, IN 47906, USA.
E-mail address: kpark@purdue.edu (K. Park).

https://doi.org/10.1016/j.jconrel.2022.08.052
Received 29 May 2022; Received in revised form 25 August 2022; Accepted 26 August 2022
Available online 6 September 2022

Semi-solvents can also be used to understand more about the microstructure (or morphology) of the microparticles, which are manifestations of using different types of PLGAs and manufacturing conditions [6,7]. These parameters can significantly affect the drug release kinetics, and studying them provides information on further characterization of PLGA microparticles. Morphological characterization of PLGA microparticles can be done using image analysis programs on electron microscopic and light microscopic images. However, investigating the changes in microparticles' surface and inner structural shape during degradation or drug release processes is challenging, especially when individual microparticles are treated with solvents, etc. Moreover, it is desired to examine morphological changes based on the same microparticle(s). This necessitated the development of a new method for examining morphological changes occurring on the same microparticle (s) during a series of sequential experimental procedures.

This study describes a new method of examining morphological changes of the same particle(s) during exposure to sequential semi-solvents in the vapor phase rather than in the liquid phase. This is similar to the absorption of water moisture into hygroscopic compounds. Microparticles made of PLGAs were found to absorb organic vapors, and, depending on the semi-solvent type, the microparticles underwent different morphological and microstructural changes. The finding that semi-solvents in the gas phase can be used to examine the semi-solvent effect enabled the development of a robust and reproducible method for understanding the microparticle compositions and microstructural arrangements that play a critical role in the performance of PLGA formulations.

2. Materials and methods

2.1. Materials

Lactide (L) and glycolide (G) monomers were purchased from Ortec. Butanone (= methyl ethyl ketone, MEK), decanol, dichloromethane (DCM), ethyl isobutyrate (EI), gelatin (type B), lactic acid, toluene (Tol), 2-pentanone (2PE), phosphate-buffered saline (PBS), PBS with 0.5% tween-20 (PBST), poly(vinyl alcohol) (PVA) (Mowiol 4–88), propyl acetate (PA), and stannous octanoate (SnOct) were purchased from Sigma Aldrich. Acetone (ACE), benzyl alcohol (BZA), hexane (HEX), methanol (MeOH), tetrahydrofuran (THF), and 20 mL glass vials were purchased from Fisher Scientific. Ethanol (EtOH) was purchased from Decon Laboratories. Naltrexone (free base) (NTX) was purchased from Spectrum Chemical Mfg. Corp. A nylon mesh filter was purchased from Component Supply Company. Calcium sulfate (Drierite) was from the W.A. Hammond company. Leuprolide acetate was purchased from Selleck Chemicals. Hexane was purified by distillation (65–85 °C), and stannous octanoate was purified by vacuum distillation at 200–250 °C and -31 inHg.

In addition to commercially procured PLGA polymers, PLGAs with specific lactide:glycolide (L:G) ratios, molecular weights, and endcaps were synthesized according to methods previously described [1,2,4–6]. Briefly, a round-bottom flask was charged with lactide, glycolide, and suitable initiator, lactic acid for acid endcap or decanol for ester endcap. The initiator was added to the monomer at a 1:200 M ratio, and the flask was vacuum purged. Subsequently, the mixture was heated to 150–170 °C for 8 h to react under a vacuum. The crude polymer was rinsed with ethanol, redissolved in DCM, filtered, and precipitated in hexane, a non-solvent for PLGA. Subsequently, the collected precipitate was dried under vacuum (−31 inHg) at 50–60 °C for 2–3 weeks until reaching constant mass.

2.2. Preparation of microparticles

Microparticles were prepared using the previously described oil/water (o/w) single emulsion method [4]. For blank microparticles, a PLGA polymer was first dissolved in 45 mL DCM at 18% (w/v). These solutions were then added through an 18 Ga needle into 4 L of 0.5% (w/v) PVA agitated with a 1/3 off-set paddle rotating at 1000 RPM and stirred for 5 h. The particle slurry was decanted through a 7 μm nylon mesh filter to collect the particles, rinsed with deionized water, collected into a centrifuge tube, and washed three times with refrigerated deionized water by centrifugation at 2000 RPM for 1 min. The collected particles were dried in a vacuum desiccator over calcium sulfate at reduced pressure (75 Torr) for 2–3 days until constant mass, then passed through an #80 mesh (< 177 μm). Particles were stored at −20 °C.

For imaging purposes, drug-loaded microparticles were prepared to examine the impact of drugs or other excipients on morphological changes. Naltrexone was used as a model hydrophobic drug [8,9]. Naltrexone was dissolved in 50 mL 9:1 DCM:ACE at the concentration of 16% (w/v). This solution was then emulsified in a PVA solution and prepared according to the same methods applied to the blank particles. An alternate manufacturing process was performed by mixing 1.35 g DCM and 0.632 g BZA. This combined solution was used to dissolve 506 mg of PLGA-75 L (Evonik, RG755S), followed by adding 270 mg of naltrexone. This solution was combined with 10 mL of 1% PVA water and homogenized for 1 min at 7000 RPM. Subsequently, the emulsion was added to 380 mL of chilled 1% PVA and stirred at 4 °C overnight. Then, the emulsion was passed through a #80 mesh and collected on top of a 7 μm nylon mesh. Subsequently, the particles were resuspended in 200 mL of 25% ethanol solution and stirred for 8 h, then collected and dried in a vacuum desiccator over calcium sulfate at reduced pressure (75 Torr) for 2–3 days [10].

For a model hydrophilic compound using a water/oil/water (w/o/w) double-emulsion method, leuprolide microparticles were prepared by previously reported methods [11–14]. A 0.1 mL aqueous solution containing 20 mg leuprolide acetate and 3.6 mg gelatin was prepared to make microparticles. In addition, microparticles containing gelatin alone (no leuprolide) were prepared. The primary emulsion was prepared by adding this aqueous solution into 0.5 mL of 384 mg/mL PLGA in DCM with vortex mixing at 0 °C. The secondary emulsion was prepared by combining the primary emulsion into 4 mL of 0.25% PVA aqueous solution with homogenization (IKA, T-25 homogenizer) at 12,000 RPM. Subsequently, the emulsion was stirred for 3 h by an overhead stirrer. The prepared particles were sieved through a #80 sieve, collected on top of 7 μm nylon mesh, washed with deionized water, and dried in a vacuum desiccator. Table 1 lists all PLGA

Table 1
PLGA microparticle formulations prepared for testing.

Formulation	Description (PLGA L:G ratio = %L*, MW*, Source)
1	PLGA-50 L (50:50 = 50 L, 60,889 Da, Evonik RG504H)
2	PLGA-75 L (75:25 = 75 L, 72,176 Da, Evonik RG755S)
3	PLGA-100 L (100:0 = 100 L, 76,276 Da, PolySciTech AP093)
4	Polylithic 50 L + 100 L (1:1 (by weight) mix of PLGA-50 L (Evonik RG504H) and PLGA-100 L (PolySciTech AP093)
5	PLGA-75 L-NTX ACE:DCM (Naltrexone-loaded PLGA (Evonik RG755S) microparticles. Naltrexone was dissolved in 9:1 ACE:DCM at the 16% concentration and emulsified in chilled 1% PVA water followed by ethanol wash. The final naltrexone loading was 3.3% (w/w).
6	PLGA-75 L-NTX BZA:DCM (Naltrexone-loaded PLGA (Evonik RG755S) microparticles. Naltrexone was dissolved in 7:3 BZA:DCM at the 35% concentration and emulsified in chilled 1% PVA water followed by ethanol wash. The final naltrexone loading was 26.1% (w/w). Duplicate lots were made using the same method to test reproducibility.
7	PLGA-75 L-LeupGel (Leuprolideand gelatin were loaded into PLGA microparticles by a double emulsion method). (PLGA 75:25 with acid-endcap, 18,938 Da from PolySciTech, AP165).
8	PLGA-75 L-Gel (Gelatin was loaded into PLGA microparticles by a double emulsion method). (PLGA 75:25 with acid-endcap, 18,938 Da from PolySciTech, AP165).

* %L was measured by HNMR, and molecular weight (MW) was measured by GPC using external standards (GPC-ES).

microparticle samples prepared for testing in this study.

2.3. Characterization of PLGAs extracted from microparticles

PLGA polymers were characterized as previously described [1,4–6]. PLGA was extracted from each microparticle sample and assayed as described [1]. Briefly, 15 mg of each microparticle batch were dissolved in 1 mL of DCM and passed through a 0.45 μm PVDF syringe filter into 10 mL of ethanol in a 15 mL glass centrifuge tube. The precipitate was centrifuged at 3300 RPM for 10 min, the ethanol was decanted, and then the collected PLGA was dried under a heated vacuum (−31 inHg, 50–60 °C). For NMR measurement, samples were dissolved in 0.8 mL of silver-foil stabilized $CDCl_3$ and put in a 7-in. NMR tube (Norell). Scans were performed at the Purdue Interdepartmental NMR Facility [15]. Briefly, NMR scans were generally performed on a 500 MHz (HNMR, Bruker DRX500-1) with 8–32 scans and a delay of 1–3 s or 800 MHz (C13NMR, Bruker Avance-III-800) instrument with 1024–4096 scans and a delay of 8–32 s. Gel permeation chromatography-external standard (GPC-ES) was performed on a Waters Breeze-2 system with a 1 mL/min THF mobile phase across three GPC columns (Phenogel 10^4 Å, 50 Å, and Agilent ResiPore) with refractive index detection and calibration against polystyrene standards (Agilent PS2). GPC-quaternary detection was performed on a Wyatt system consisting of an Agilent 1260 Infinity II front end connected to a Wyatt Dawn Heleos II (multiangle light scattering), Viscostar III (viscometer), Optilab T-rEX (refractive index), and Dynapro Nanostar (dynamic light scattering) detectors. Separation was performed using 0.6 mL acetone across a linear gradient column (Tosoh Bioscience, TSKGel GMHHR-7), and the instrument was normalized using poly(methyl methacrylate) standards.

2.4. Differential scanning calorimetry

The prepared microparticles were tested by differential scanning calorimetry (DSC) to obtain their thermal properties. This was done using an MDSC Q2000 (TA Instruments). Modulated DSC was performed on samples (2–5 mg) in aluminum pans under 50 mL/min argon flush by setting a program to equilibrate to −80 °C, modulate ±1 °C every 30 s, hold isothermal for 5 min, and ramp at a rate of 3 °C/min to 200 °C.

2.5. Microparticle surface analysis

Three-dimensional (3D) images of microparticles were obtained using a laser scanning confocal microscope (LSCM) (LEXT® OLS5000 from Olympus) equipped with 5×, 10×, LM-20×, LM-50×, and LM-100× objectives and a motorized stage. The imaging was performed in a low-vibration condition, including a vibration isolation platform (VIBe Mechanical) under the microscope on a sturdily mounted table directly on concrete slab foundational flooring in a room with orange-filtered lighting and no prevailing air currents. The instrument was operated, and scan files were processed using Olympus OLS5000 software. Thermal control was provided by either a Peltier stage cooler (Linkham model PE120) or by recirculating fluid (ThermoNeslab digital-one recirculating chiller) passed through a plumbed conductive plate (Lytron, P/N CP12G05).

Preliminary testing established a few parameters critical for successful LSCM imaging. A non-reflective (either dark or clear) background improved the imaging quality. LSCM can measure the top of the particles but cannot examine the bottom and sides as the laser is blocked by the top of the particles (i.e., the shadow effect). Additionally, clumps of aggregated particles tend to interfere with measurements of individual microparticles. In addition, the image quality was reliant on the scan setting (e.g., fast, standard, or fine) and the magnification of an objective applied. Laser scanning on particles under the liquid solvent or a glass coverslip is inhibited due to the interfering refractive properties of the media the laser passes through. Although sufficiently heavy or frictional objects will move in tandem with the motion of the motorized stage, the incidence of slip between the object and the stage decreases the resolution of the fine motion for lighter objects.

2.6. Application of sequential semi-solvents

Microparticles were treated with a sequence of semi-solvents, chosen first to dissolve PLGAs with a higher lactide content. Each semi-solvent was removed before the application of the next. The impact of each semi-solvent on microparticle surface morphological changes was examined. A residual solvent may likely remain after each semi-solvent treatment even after overnight drying, and it may affect the microstructure, which depends on the formulation's composition and manufacturing process. It is such an impact on the microstructural change that allows comparison of different microparticles as long as the same experimental procedure is applied. Two different methods were examined for the sequential semi-solvent treatment as described below.

2.6.1. Application of semi-solvent liquids in sequence

Microparticles were secured on the surface when liquid semi-solvents were introduced sequentially to prevent movements and potential loss of particles during the removal of each solvent. Initially, two different methods were tested: channel and glue methods. In the channel method, a slab of brass metal was machined to contain an array of 4 × 13 × 1 mm^3 channels arranged in triplicate in a series of quadrants. A central hole was drilled to allow for mounting of the slab directly to the OLS5000 robotic stage via threaded mounting holes (metric size M4). Particles were sprinkled across each quadrant through an open-mesh sieve (~2 mm) and then exposed to select solvents by pipetting the solvent into the respective well for 1 min at room temperature, followed by solvent removal via pipette and drying under a fume hood overnight. Selected microparticles from each well were scanned via LSCM.

Semi-solvents dissolve PLGA only if the polymer has a molar lactide content above a specific cut-off value. In this study, semi-solvents were selected based on their cut-off solubilization properties of PLGA. For quantification of semi-solvents, this cut-off is defined as $L_{10mg/mL}$, which is the minimum lactide content necessary for the solvent to dissolve a 10 mg/mL concentration of the PLGA at a fixed molecular weight of 80 ± 20 kDa. For example, a solvent with a 75% $L_{10mg/mL}$ value would easily dissolve PLGA 85:15 but has poor solubility for PLGA 70:30. Semi-solvents serve as a powerful analytical tool, and they have been characterized in great detail as part of previous studies [6].

In the glue method, microparticles were secured to the surface using light-cured glue. For each sample, a 3″ x 1″ microscope slide with embedded gridlines (Research Products International, cat# 160244) was prepared to place a thin layer of photocurable adhesive (Loctite 3494) along one side. A razor blade was used to wipe the adhesive out as a thin layer across the surface of the slide and allowed to dry for 5 min. The sample particles were sifted carefully through a mesh onto the grid slide. Then the glue was activated by exposure to UV light inside a UV Curing chamber (Loctite, Zeta 7401) for no >10 s to prevent microparticle damage due to heat. Six particles were imaged by LCSM at 100× magnification in fine scanning mode, and their exact locations on the grid were recorded so they could be located later. All solvent exposure work was conducted under argon flush in the presence of desiccant to prevent humidity-associated complications. As shown in Fig. 1, a syringe pump attached to a self-centering blunt-tip needle was utilized to add 0.3 mL of pre-chilled solvent at 1 mL/min. The solvent was allowed to remain for 1 min, and then the pump was utilized to withdraw the solvent at the same rate of 1 mL/min. Each sample was exposed to either xylene ($L_{10mg/mL}$ = 92% L), propyl propionate ($L_{10mg/mL}$ = 80% L), methyl-tetrahydrofuran (MTHF, $L_{10mg/mL}$ = 70% L), cycloheptanone ($L_{10mg/mL}$ = 59% L), or 2-butanone (MEK, $L_{10mg/mL}$ = 51% L). Subsequently, the sample was kept under argon flush for an additional 10 min before being transferred to dry in a vacuum desiccator over $CaSO_4$ at reduced pressure (75 Torr) for 1–3 days. After solvent exposure and drying, the slides were then imaged again by LCSM to obtain post-

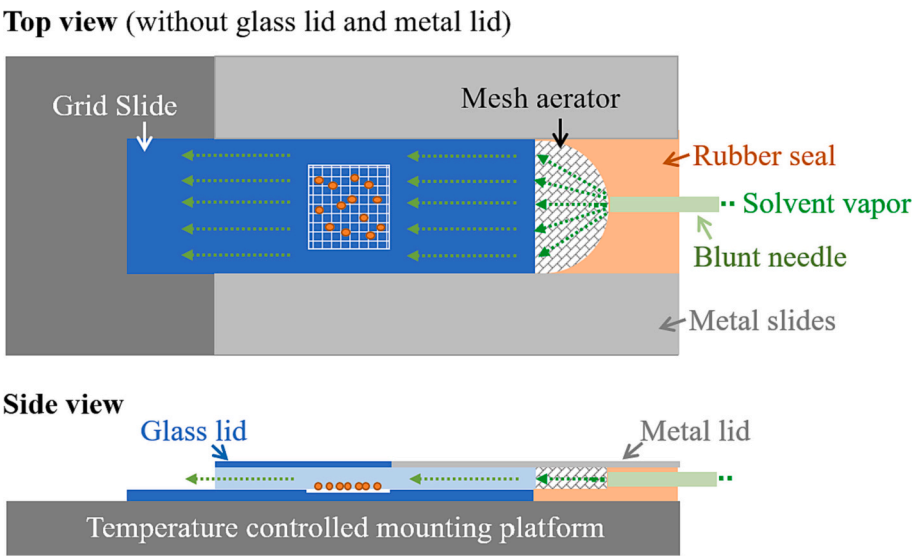

Fig. 1. A schematic overview of the semi-solvent vapor (SSV) flow-cell.

solvent images.

2.6.2. Application of sequential semi-solvent vapor (SSV)

Dry microparticle samples (~1 mg) were sifted through a 330 μm opening stainless steel wire mesh (Internet Products) mounted 5 cm above a grid-lined 3"x1" microscope slide with constant agitation provided by a titer plate shaker (Barnstead International, Model 4625) set to a speed of 2–3 on the instrument dial. This left the particles as a fine, loose dusting across the slide, enabling easier visualization and testing. The LSCM motorized stage with a custom mount consisted of a plumbed temperature control flow plate (Lytron, P/N CP12G05) bolted to the stage and connected to a separate recirculating chiller (ThermoNeslab digital-one recirculating chiller) by a length of flexible latex-rubber tubing (B&K LLC, 3/8″ x 1/4″) to allow free motion of the stage. On top of the temperature control plate, a darkened brass (surface treated with Brass Ager solution) mounting plate was connected to a custom-made horizontal gas flow diffuser. The diffuser provides gas flow from a blunt-tip needle and across a 2.5 cm wide wire-mesh aerator along the distal edge of the 1″ x 3″ inch gridded microscope slide. The gas was directed across the surface of the slide on the grid lines with a flow gap of approximately 1 mm as covered by a glass lid applied during the gas flow operation. The glass slide was securely mounted with a retaining clip to the bolted plate to prevent movement relative to the motorized stage (Fig. 1). For safety, an activated charcoal gas absorber (Valtcan, model 496) was placed adjacent to the solvent flow outlet side of the stage at a distance suitable to absorb excess solvent fumes but not interfere with any of the particle interactions or robotic stage motion.

A series of 40 mL septa-capped screw-top vials (Scientific Products LLC, P/N: 40C-TOC/dB) were charged with 10 mL of a solvent (~¼ full). The solvents used were (in the order of application) ethyl isobutyrate, toluene, 2-pentanone, and propyl acetate. These solvent bottles were mounted upright inside a digital incubator (Quincy Labs, Model 12E). The blunt needle of the SSV flow cell was attached to an 18-gauge needle using PTFE tubing (Cole-Parmer, P/N: 06417–31). Additionally, argon gas (Indiana Oxygen Company) was provided through a pressure regulator (Fisher Scientific) and an adjustable flow regulator (Dwyer) and piped through latex tubing to a 4-in. 18 Ga hypodermic needle. The temperature of the water circulator was set to 31 °C, which corresponded to a mounted surface temperature of 30 °C as verified by an external thermocouple. The difference was due to conductive heat loss. The incubator containing the solvents was heated to 40 °C. Both systems were allowed to warm and equilibrate for at least 30 mins before initiating vapor exposure. The LSCM mapped the dry particles under 5× magnification to identify particle locations. Initial experiments determined that the SSV process does not move the particles, unlike the liquid solvent method. As long as all components were securely fastened to the motorized stage, the location of specific particles was consistent. A series of microparticles on a slide were identified, and their coordinate locations were programmed into the microscope acquisition software. These were then scanned at 50× magnification in 'fine' mode with preference given to particles not close to, or clumped with, other particles to avoid interference with the imaging process, and preferentially on the right-hand side of the grid. Scanning was performed full z-axis to measure the microparticle height relative to the glass slide they were resting on, i.e., the microparticle height is equal to the diameter for spherical microparticles.

After scanning the locations of microparticles, a glass lid was slid over the grid slide. The argon gas input needle was pressed through the septa-cap of the respective solvent bottle and threaded to the bottom of the vial to bubble argon gas through the solution. The outlet syringe needle (leading to the vapor flow cell) was pierced into the septa cap at a shallow distance of ~2 cm deep (~5 cm above the fluid level of the solvent). Argon gas flow was initiated and controlled at a consistent rate of 40 cc/min for 10 min before being shut off, and both needles were removed. Subsequently, the glass cap was removed from the vapor chamber, and the same coordinate-location programmed particles were scanned by LSCM. After scanning, the cap was replaced, and the process was repeated with the next semi-solvent. The semi-solvents were exposed in the order of ethyl isobutyrate, toluene, 2-pentanone, and propyl acetate. After all solvents were processed, the slide was remapped at 5× to observe significant changes across the particles.

2.7. Image processing

The collected 3D scans were processed using LEXT analysis software (Olympus). The LEXT software (Olympus) converted the 3D scan images into quantifiable values commonly used in surface roughness profilometry [16]. Each scan had a software autocorrect function performed to fill in gaps, remove spike noise, and eliminate tilt if present. For spherical microparticles, the autocorrect function filled the particle's sides and bottom with a straight drop. Since this result is consistent across all microparticles, it was kept in this form for further processing. The region of interest (ROI) for measurement was set on top of the particle. Because the exact 'edge' of the particle that should or should not be included in the ROI is not consistently clear, each particle had three ROIs set across the entire particle surface to include nearly all of

the particle edges. Subsequently, the results were averaged to reduce the user-subjective input for which portion of the particle to measure. The average of the three ROIs on the same particle was treated as a singular data point. A spherical form factor correction was applied to reduce the effect of the natural, spherical, slope of the particle with a circular ROI, which is defined to extend slightly past the edges of the particle to ensure the entire particle has a spherical form-factor correction in place. Based on experimental optimization, the S filter (small-feature removal) was set to 1 μm (consistent with the general imaging resolution limits at the selected magnification). The L-filter (large-feature removal) was set to 50 μm, consistent with the average size of a microparticle itself. The correction type was set to Spline, and the parameter calculations were performed to obtain surface roughness and feature characterization properties. In addition to the surface roughness profilometry, dimensional aspects (surface area, area, and height) of the microparticles were collected by applying the volume threshold measurement of the LEXT software. The threshold cut-off was set to match the height of the glass surface background of the image. When necessary, ROI selections were performed to eliminate any features not attributable to the particle (e.g., other particles or parts of particles that extended into the image frame). In the case of the particle melting broadly under solvent effects, the best estimate of the particle region was used for particle volume and surface area measurements.

2.8. Statistics

Statistical comparisons between quantitative image data were conducted using an unpaired *t*-test by the GraphPad program [17]. Significance was defined as *p*-values of <0.05, <0.01, and < 0.0001 which were denoted with *, **, and ***, respectively.

3. Results

3.1. Optimization of image analysis parameters

The primary utilization of surface profilometry is to assay metal parts collected from industrial sources to evaluate their degree of wear and tear. Naturally, the conventional settings for such a methodology readily apply to the analysis of PLGA microparticle images. For optimization of appropriate optical profilometry settings, four images of four formulations were selected representing specific appearances based on particle disposition. All images were selected from particles tested using the SSV method after exposure to all solvent vapors. The images were selected from Formulation 2 (PLGA-75 L), which merely melted to a smooth surface. Formulation 4 (Polylithic 50 L + 100 L) had a highly heterogeneous surface due to the mixing of PLGA 50 L and PLGA 100 L, which have different solubilities in different semi-solvents. Formulation 6 (PLGA-75 L-NTX BZA:DCM) presented a porous surface, and Formulation 7 (PLGA-75 L-LeupGel) showed a bumpy surface (Fig. 2).

The sample images were prepared as described in Section 2.7 with autocorrection. To reduce the impact of subjective ROI selection by a user, 3 ROIs were selected on each particle by the user and averaged to create one measurement. A series of filters, including spherical form factor (removes spherical shape), S-filter (removes features below an indicated size), and L-filter (removes features above an indicated size), were tested in both Gaussian and Spline filter settings.

LEXT image analysis program has dozens of default parameters. The first necessary task was to find out which parameters were most relevant to the analysis of the surface morphology. A starting point was to find parameters that match our visual observations. Various parameters individually and as a group were examined to best represent changes in the visual observations, i.e., to convert the image data into quantifiable parameters. The LEXT program provided a multitude of profilometry and roughness characterization data rapidly. This data, however, was of limited use due to a few critical issues. Profilometry, in general, is ideally applied to flat, metallic surfaces on machined parts in an industrial setting. Other applications require substantial process modifications. The spherical nature of the particles contributes significantly to the measurement results; thus, it must be eliminated using a form-factor correction. Multiple measurements of the same microparticle with different, overlapping ROI should lead to the same measurement. However, some results obtained from the same microparticle were orders of magnitude different from one another based on whether an indeterminant edge portion was included or excluded from the measurement, even if the ROIs overlapped >90% of the selection area. This introduces a non-trivial degree of variance based on the user's subjective interpretation of the particle.

To optimize the measurement method, a single parameter, Sa (arithmetical mean height), was utilized. This parameter, which indicates the relative degree of change in height, is considered a direct measurement of the “roughness” of a surface in the most simplistic term. To the human eye, the variations in what a particle ‘looks’ like in the provided laser scans are instantly apparent in the basic description. Indeed, a user aware of the particle type can readily identify features, such as the cubic crystals of naltrexone or the bumps of gelatin double emulsion poking up through the vapor-melted particle substrate. A

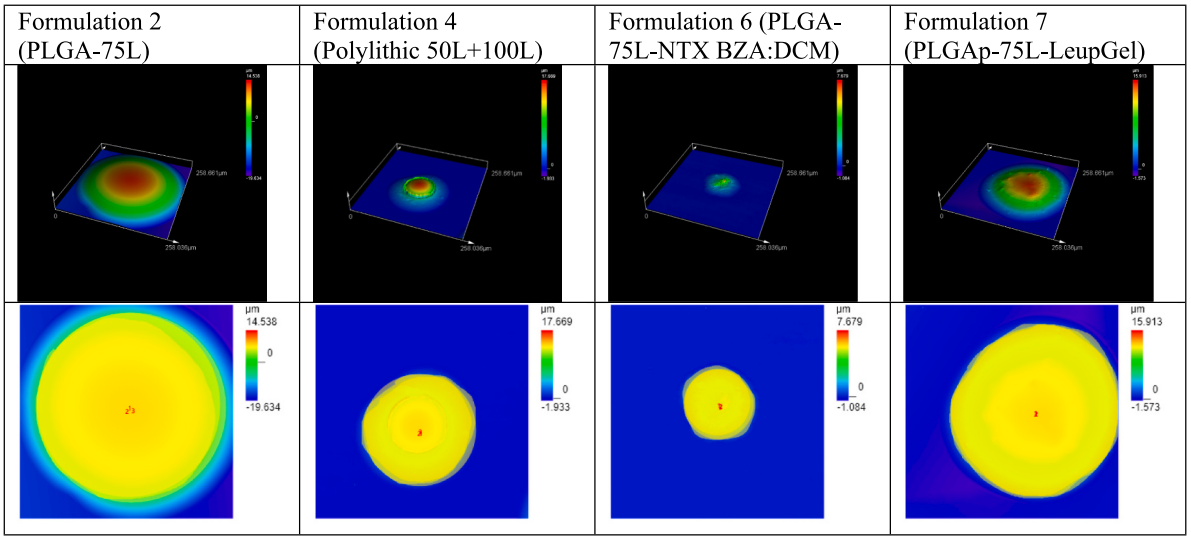

Fig. 2. (Top row) Selected images representing specific, observable features of different formulations after exposure to all semi-solvent vapors. (Bottom row) Selected images showing the region of interest (ROI). ROI areas are highlighted with a yellow color overlaying on the height map's top.

series of particle scans identified visually as smooth, porous, bumpy, and heterogeneous were used for this optimization work. For all measurements, the spherical form factor was applied. For each particle, three overlapping regions of interest were placed over the entire particle surface to the best of a user's ability. S-filter (λs filter or low-pass filter) eliminates the smallest scale elements (e.g., noise) from the surface. L-filter (λc filter or high-pass filter) eliminates the largest scale elements from the surface, i.e., removing undulations and other lateral components. F-operator (λf filter) removes form from the primary surface for tilt correction, allowing nominal surface texture characterization. Additionally, either "Gaussian" or "Spine" filter mode was selected. Gaussian filter is an iterative algorithm that weights data points based on a wave profile, while the Spline filter applies geometrical smoothing to curves that interpolate adjacent data points [18]. The functional parameters included lower roughness values measured for the visually smooth particle compared to the porous and bumpy heterogeneous particle with the highest roughness value. Since both porosity and bumpiness contribute to overall height variations, no substantial difference in Sa is expected. This is because the calculation is based on absolute value and makes no distinction between the mathematical height contributions of portions extending outward from a surface versus those extending inward from the same surface. Additionally, the relative standard deviation of the triplicate ROIs for each particle type should be minimized, indicating a reduced variance caused by user input. Table 2 below shows the selected Sa (arithmetical mean height) measurements representing surface roughness.

If filters were not applied, the smooth particle readily relays a higher roughness measurement than the visually porous particle due to the particle's large, general slope even after removing the form factor. Of the various filters applied, the S = 1 μm and L = 50 μm in Spline mode provided the most reasonable results relevant to visual observation (roughness of smooth < porous ~ bumpy < heterogeneous) and the lowest RSD for triplicate measurements. The lower value of 1 μm is comparable to the resolution limits of imaging at this magnification. The higher value of 50 μm appears reasonable as it corresponds to roughly the average size of the particle itself. For quantifications, this filter set was applied consistently.

3.2. Quantitative analysis of SSV impact on the selected microparticle sets

Several of the many parameters available in the LEXT program are either interdependent or interchangeable. One parameter can be selected for interchangeable parameters to have better coverage of the morphology. Height parameters are known to examine surface roughness. Sa (arithmetical mean height) and Sq (root mean square height) are widely used because they represent surface morphology. Since Sa and Sq have a strong correlation, only one can be used [19]. Our preliminary studies showed that the surface morphological changes of PLGA microparticles could be described using the following parameters (Table 3): Sa (arithmetical mean height), Sz (maximum height), Ssk (skewness), Sku (kurtosis), Sal (auto-correlation length), Vmc (core material volume), Sk (core roughness depth), and Hm (maximum height from glass threshold) [20]. Rs (shape ratio) was also used to describe the melting/collapse of PLGA microparticles, leading to spreading on the glass surface after exposure to semi-solvents.

Table 2
Sa (arithmetical mean height) measurements of three ROIs of the same microparticle with indicated filter settings.

Sample (description)	No S/L Filter	S = 2 μm, L = 20 μm (Gaussian)	S = 2 μm, L = 20 μm (Spline)	S = 1 μm, L = 50 μm (Spline)	S = 1 μm, L = 100 μm (Spline)
Smooth (75 L Blank)	0.390 ± 0.083	0.006 ± 0.001	0.005 ± 0.000	0.014 ± 0.001	0.052 ± 0.006
Porous (75 L + NTX)	0.291 ± 0.020	0.114 ± 0.008	0.119 ± 0.008	0.193 ± 0.012	0.248 ± 0.019
Bumpy (Leuprolide)	0.674 ± 0.010	0.050 ± 0.007	0.052 ± 0.008	0.157 ± 0.011	0.301 ± 0.014
Heterogeneous (50 L + 100 L)	2.545 ± 0.082	0.271 ± 0.011	0.283 ± 0.012	0.699 ± 0.025	1.445 ± 0.053
Average relative standard deviation	8%	12%	6%	5%	7%

3.3. Characterization of PLGA polymers

PLGA polymers extracted from microparticle formulations were characterized to determine their properties by NMR and GPC-4D. This information helps understand the different responses of microparticles to the same SSV treatments. Table 4 below displays the resultant data.

DSC was used to measure the glass transition temperatures (T_g) and drug melting transitions of the respective formulations in the dry and wet states. The dry microparticles were soaked in PBS for 30 min, and the excess water was removed while still partially damp. Water is quickly uptaken into PLGA microparticles [3], and water serves as a plasticizer for the PLGA chains, typically affecting the glass transition of the formulated microparticles [22]. The degree to which this occurs depends on microparticles' components and microstructural properties. Table 4 also lists the measured T_g values. The T_g values decreased upon wetting for all formulations except the 100 L (PLA), which did not change, likely due to the higher hydrophobicity of PLA [23].

3.4. Surface analysis of microparticles after exposure to semi-solvent liquids

A semi-solvent can dissolve at least 10 mg/mL of a PLGA (~80 kDa)

Table 3
Parameters used for evaluating surface morphology [20,21].

Parameter	Property
Sa (μm)	Arithmetical mean height: The absolute height difference was measured to determine the average difference in height for every point relative to the mean plane of the surface.
Sz (μm)	Maximum height is the sum of Sp (maximum peak height) and Sv (maximum pit height).
Ssk	Skewness represents the deviation of the peaks and valleys (unevenness) on the surface with reference to the mean line of a profile curve. It indicates whether the surface is smoother with less removal of materials and narrow valleys (Ssk < 0) or a sharper surface with more removal of materials and wide, deep valleys ((Ssk > 0).
Sku	Kurtosis represents the sharpness of the peaks and valleys (unevenness) on the surface with a value of <3 for smoother peaks and wide valleys and with a value >3 for sharper peaks and narrower valleys.
Sal	Auto-correlation length measures surface texture by identifying surface features and evaluating the periodicity of each surface direction. The low Sal value indicates the surface with a uniform pattern in the horizontal direction, and the higher Sal value for a spatially random pattern
Vmc	Core material volume is used to obtain the volume of the material present within the areas, excluding extreme peaks and valleys.
Sk	Core height is the height for the core surfaces, excluding the extreme peaks and valleys.
Hm	Maximum height of microparticles from the threshold (i.e., the height of the glass slide). This value simply measures how tall a particle is on a glass slide. One advantage of this parameter is that it requires no data processing, such as applying filters and assuming a spherical shape.
Rs	Shape ratio: The ratio of the 3-dimensional particle surface area divided by the contact area between microparticles and glass surfaces. Initially, microparticles are in contact with the surface only at the microparticle bottom; thus, Rs is large. As microparticles melt and collapse/spread upon exposure to semi-solvents, the contact area with the glass surface increases, decreasing the Rs value. Both Hm and Rs describe the particle melting property effectively.

Table 4
Characterization of PLGAs extracted from microparticle formulations.

			GPC-4D					T_g (°C)	
Formulation	Description	L% (HNMR)	M_n	M_w	PDI	Solvation radius (nm)	Intrinsic viscosity (mL/g)	T_g (Dry)	T_g (Wet)
1	PLGA-50 L	50.0%	39,476	48,929	1.24	6.59	37.69	27.6	19.7
2	PLGA-75 L	75.2%	33,941	41,799	1.23	6.60	40.14	32.1	24.8
3	PLGA-100 L	100.0%	39,293	55,186	1.40	6.95	46.57	39.8	40.3
4	Polylithic 50 L + 100 L	73.7%	39,880	52,256	1.31	6.40	41.58	32.6	25.5
5	PLGA-75 L-NTX ACE:DCM	75.1%	32,134	39,079	1.22	6.87	38.46	51.2	35.9
6	PLGA-75 L-NTX BZA:DCM	74.9%	21,846	28,127	1.60	1.6	31.6	51.3	47.8
7	PLGAp-75 L-LeupGel	75.1%	17,067	18,804	1.10	4.13	23.19	51.0	33.2
8	PLGA-75 L-Gel	75.0%	17,249	19,398	1.13	4.11	22.77	50.9	32.6

if the PLGA has a lactide content above the minimum threshold ($L_{10mg/mL}$). Thus, using different semi-solvents in sequence allows the dissolution of PLGAs based on their lactide contents. Surface analysis after sequential semi-solvent impact (SASSI) was conducted by exposing PLGA microparticles to different semi-solvent liquids. The particles needed to be secured on the surface to observe the morphological changes of the same microparticles. Initially, the channel method was used. The flat brass surface was striated to hold microparticles in confined channels and introduce semi-solvents. When semi-solvent was added to the microparticles in the striated channels, the particles tended to clump if the semi-solvent was a poor solvent for PLGA, e.g., 2-pentanone ($L_{10mg/mL} = 69\%$) for Formulation 1 (PLGA-50 L), or microparticles became melted very quickly, e.g., 2-pentanone and butanone (MEK) ($L_{10mg/mL} = 51\%$) for Formulation 2 (PLGA-75 L) particles. The introduction and removal of each semi-solvent resulted in removing microparticles from the viewing area and changing the orientation even if microparticles remained in their positions.

The glue method was adopted to secure microparticles on the surface more firmly. The microparticles were evenly spread across an extremely thin layer of photo-adhesive glue on a glass slide and cured with minimal exposure. Excess glue easily embedded the particles too deep, interfering with the assay, and also damaged the particles by heat exposure from the UV-curing oven. A series of slides were produced with microparticles secured on a very thin glue layer for image analysis. In situations where the glue had an effect, it manifested in the images as ripples on the surface of the background slide and a ring around the particle (Fig. 3, top images). The glue method provided significant formulation differences. PLGA 75 L (Formulation 2) exhibited little impact from xylene solvent exposure. In contrast, the polylithic particle (Formulation 4) exhibited dissolution of only PLGA 100 L, leading to a heterogeneous appearance with large, gaping holes. However, two different PLGA-NTX formulations (Formulations 5 and 6) did not exhibit appreciable differences. Both largely melted and dissolved quickly in the solvents, with little usable differences observed in their behavior (Fig. 3, bottom images).

These tests relying on semi-solvent liquids indicated several drawbacks. Both the channel and glue methods present reliable handling challenges as the liquid exhibits a specific flow pattern only wetting across certain portions of the surface, applying shear forces against the particles in a directional fashion, and inability to completely remove the solvent by pipetting or other techniques. Thus, removing the solvent required drying the particles under a vacuum for at least a day, depending on the solvents' boiling point. Overall, the microparticles had to go through many time-consuming steps that could potentially alter the surface morphology. Because of these issues, a different technique that does not utilize liquid solvent exposure was developed. After two years of study dealing with semi-solvents in the liquid phase, a simpler method was developed using the semi-solvent in the vapor phase.

3.5. Surface analysis of microparticles after exposure to sequential semi-solvent vapors (SSVs)

It was found that the semi-solvents in the vapor phase could dissolve PLGAs, as the semi-solvents in the liquid phase. The semi-solvents used

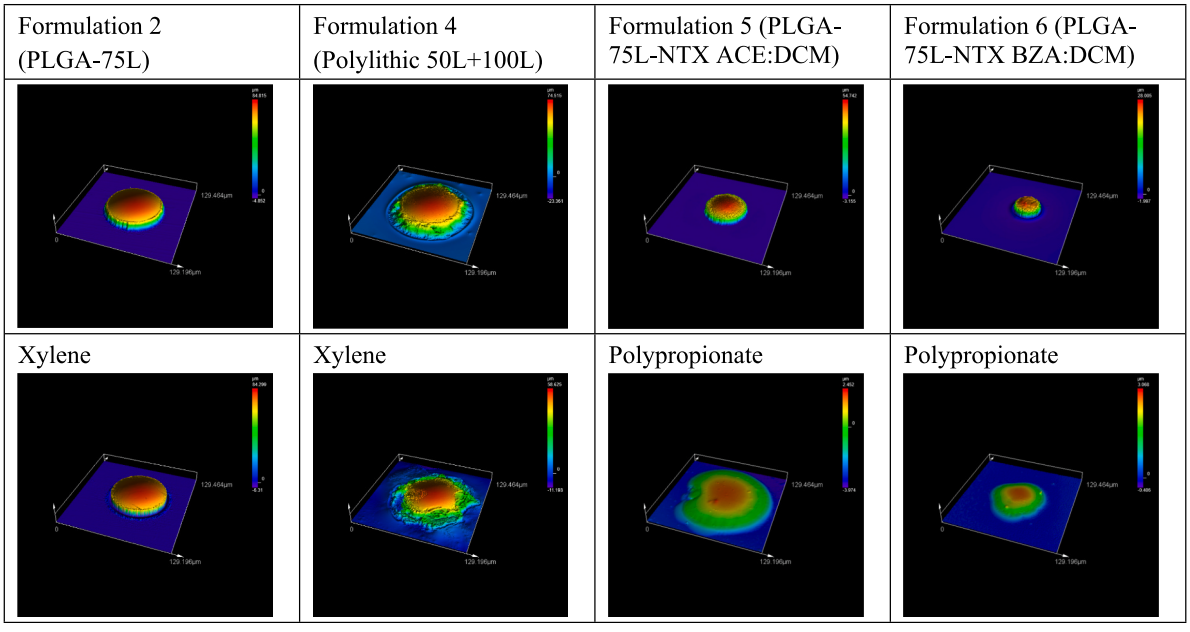

Fig. 3. Microparticles of different formulations in the dry state (top panel) and after exposure to a semi-solvent liquid at 0 °C for 1 min.

in the vapor phase differed from those in the semi-solvent liquid method because of the need for sufficient solvent vapor formation. The semi-solvents used were ethyl isobutyrate, toluene, 2-pentanone, and propyl acetate, as listed in Table 5. For obtaining sufficient quantity in the vapor phase, semi-solvents with relatively low boiling points at around 100–110 °C were chosen. At 40 °C, those semi-solvents produced enough vapor for partially dissolving PLGAs depending on their L:G ratio. The minimum lactide% ($L_{10mg/mL}$) that allow dissolution in semi-solvents are 85%, 78%, 69%, and 63% for ethyl isobutyrate, toluene, 2-pentanone, and propyl acetate. This concept is explained in Fig. 4. Ethyl isobutyrate can dissolve PLGAs only if the L:G ratio is 85:15 or higher, as indicated by the purple color in Fig. 4. Likewise, toluene can dissolve PLGAs only if the L:G ratio is 78:22 or higher. Thus, by treating PLGA microparticles with ethyl isobutyrate, toluene, 2-pentanone, and propyl acetate in sequence, only selected PLGAs in microparticles can be dissolved. Such dissolution can affect the microstructure, resulting in altered morphology. Such change can be easily identified visually, as well as quantitatively.

In the semi-solvent vapor (SSV) method, the slide was not removed from the microscope during the procedure, and only the SSV was introduced to the glass surface. Our initial tests indicated that the airflow did not produce enough shear force to move the particles. Thus, the process could be semi-automated by preprogramming in particle locations and letting the software scan the particles without directly handling the slide. This eliminates the need to glue the particles down and another source of variability for rapid and routine profiling of a larger number of particles (N = 10–20). This process enabled each particle to go through exposure to a sequence of semi-solvents to track the changes upon solvent exposure. Fig. 5 shows images of 8 formulations in Table 1 before and after SSV treatments.

Visual examination of images in Fig. 5 indicates different responses to the same SSV treatments depending on the formulation. Formulations 1–4 exhibited melting behavior corresponding to the PLGA type. Formulation 1 (PLGA-50 L) did not change upon exposure to all 4 solvents. Formulation 2 (PLGA-75 L) exhibited partial melting in toluene, and the highly melted composition started from exposure to 2-penanone ($L_{10mg/mL}$ of 69%). Formulation 3 (PLGA-100 L) exhibited collapse from exposure to the first solvent, ethyl isobutyrate, with $L_{10mg/mL}$ of 85% [6]. Formulation 4 (Polylithic 50 L+ 100 L) consists of two PLGAs, 50 L and 100 L, and only PLGA 100 L responded to semi-solvents.

Formulations 5 and 6 are naltrexone formulations prepared using a combination solvent of ACE:DCM and BZA:DCM, respectively. The two formulations exhibited very different responses when exposed to the same sequential solvent vapors. As shown in Table 4, Formulation 6 exhibited a more significant molecular weight decrease than Formulation 5. This may have affected the structure of microparticles, altering the responses to SSVs. Naltrexone is known to degrade PLGAs [10,24–26], and the higher naltrexone loading in Formulation 6 (26.1% w/w) than in Formulation 5 (3.3%, w/w) may have been a factor. The decrease in molecular weight coupled with the higher naltrexone loading may have resulted in a more rapid collapse by exposure to SSVs than that generally encountered for PLGA-75 L in Formulation 2. An important point here is that SASSI-SSV can detect the difference in formulation parameters, drug loading, and manufacturing processing parameters between Formulations 5 and 6.

Table 5
Solvent exposure sequence and solvent properties.

(Order) Solvent	$L_{10mg/mL}$[1]	Boiling Point[2]	Vapor Pressure[2]	Mass volatilized (n = 3)[3]
(1) Ethyl Isobutyrate	85%	112 °C	40 Torr (34 °C)	86 ± 1 mg
(2) Toluene	78%	110 °C	22 Torr (20 °C)	78 ± 3 mg
(3) 2-pentanone	69%	101 °C	27 Torr (20 °C)	97 ± 9 mg
(4) Propyl acetate	63%	102 °C	25 Torr (20 °C)	113 ± 4 mg

[1] The minimum lactide% of PLGA to dissolve in semi-solvent to 10 mg/mL at 30 °C.
[2] Published data from www.Aldrich.com.
[3] Conditions: 40 cc/min argon, 40 °C incubator, 10 min. Determined gravimetrically.

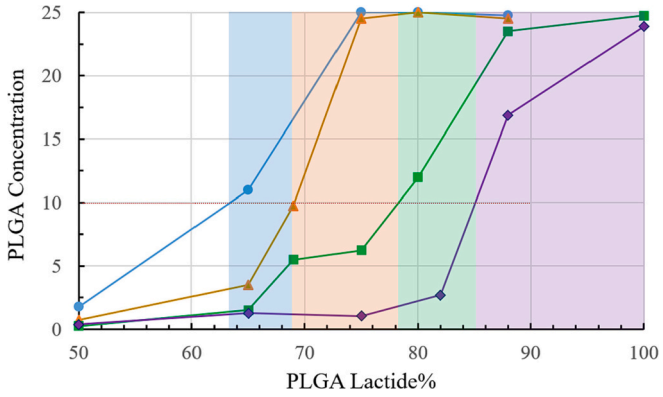

Fig. 4. Dissolution of PLGAs as a function of the L:G ratio in different semi-solvents, ethyl isobutyrate (◆), toluene (■), 2-pentanone (▲), and propyl acetate (●).

Formulations 7 (PLGA-75 L-LeupGel) and 8 (PLGA-75 L-Gel) both exhibited a bumpy surface as the gelatin granules (insoluble in all organic solvents) began poking up out from the melting PLGA particle in the late stages of vapor exposure. Formulations 7 and 8 (prepared by a w/o/w double-emulsion method) exhibited a highly different morphology upon solvent exposure than Formulations 5 and 6 (prepared by an o/w single emulsion method). Such difference results from the nature of the drugs loaded in the microparticles. Naltrexone, a small hydrophobic drug, is incorporated directly into the polymer solution (as in amorphous solid dispersions). In contrast, the hydrophilic leuprolide with gelatin as a stabilizing protein is incorporated through a double emulsion method. Thus, as a portion of PLGA in the microparticles dissolves/melts, the leuprolide/gelatin particles remain intact, leading to the overall bumpy appearance. This difference highlights one of the capabilities of this method to reveal internal structures not readily determined by other methods. Interestingly, Formulation 7 microparticles exhibited, at least initially, a degree of resistance to melting upon exposure to semi-solvents relative to Formulation 8. This may be due to the ionic interaction between polymer and leuprolide, which may strengthen the structure [11,27].

While visual observation identifies different responses of the formulations to SSV exposure, it is still qualitative. Thus, the visual information was converted to quantitative values using selected parameters described in Table 3. Ten microparticles of each formulation were assayed after exposure to each semi-solvent to quantitate the surface morphological changes, as described in Table 6.

The changes in the 9 parameters in Table 6 match with visual observations in Fig. 5. For example, the parameter values for Formulations 1–3 in Table 6 match the formulation images in Fig. 5. Formulation 1 (PLGA-50) is microparticles of PLGA 50:50 without any drugs. Table 5 and Fig. 4 show that PLGA 50:50 did not dissolve in any semi-solvents. This is reflected in the values of the nine parameters that remained the same after SSV treatments. Formulation 2 (PLGA-75 L) showed a significant decrease in Sa and Rs after treating ethyl isobutyrate** and toluene***. As expected, the changes across several other parameters became pronounced after exposure to 2-pentanone. Similarly, Formulation 3 demonstrates a significantly decreased Rs after exposure to ethyl isobutyrate relative to Formulation 2*** as the PLGA 100 L microparticles readily dissolve in semi-solvents.

Of the 8 formulations, one parameter alone (e.g., Sa, Hm, or Rs) can

Formulation	Semi-solvent Applied				
	None	Ethyl isobutyrate	Toluene	2-Pentanone	Propyl acetate
1. PLGA-50L	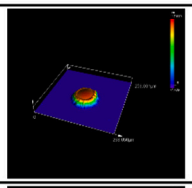	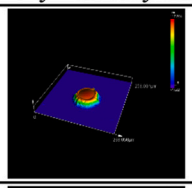	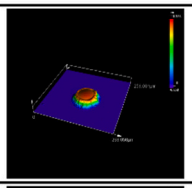	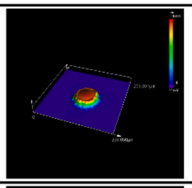	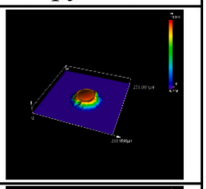
2. PLGA-75L	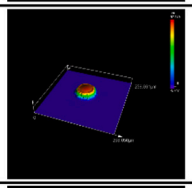	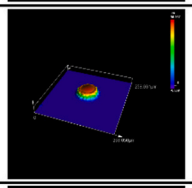	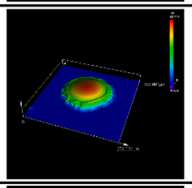	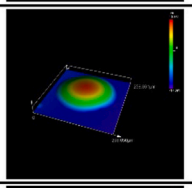	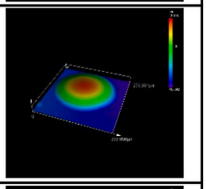
3. PLGA-100L	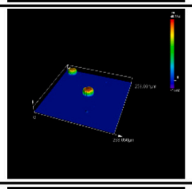	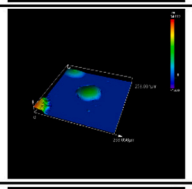	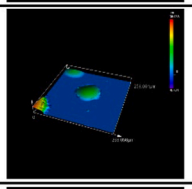	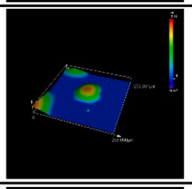	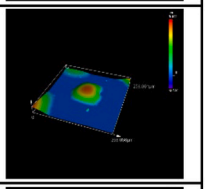
4. Polylithic 50L+ 100L	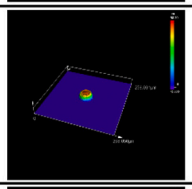	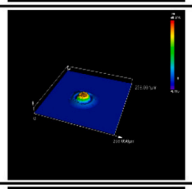	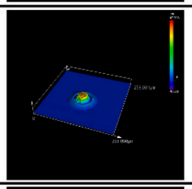	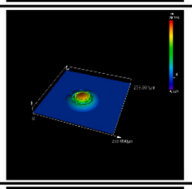	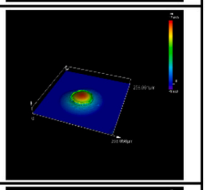
5. PLGA-75L-NTX ACE:DCM	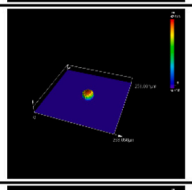	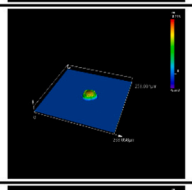	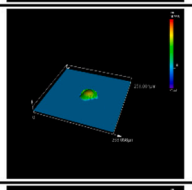	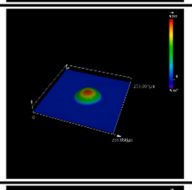	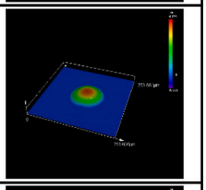
6.1 PLGA-75L-NTX BZA:DCM	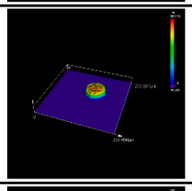	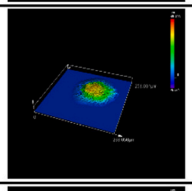	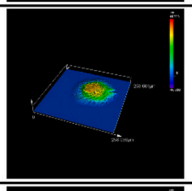	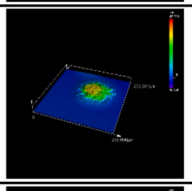	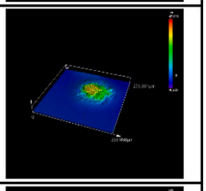
6.2 PLGA-75L-NTX BZA:DCM	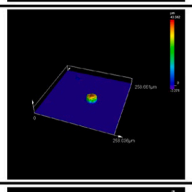	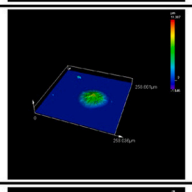	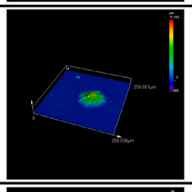	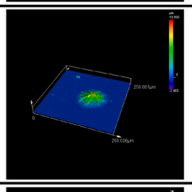	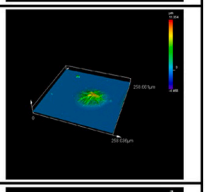
7. PLGAp-75L-LeupGel	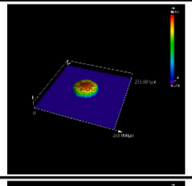	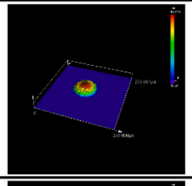	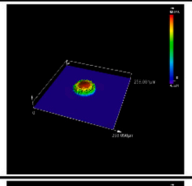	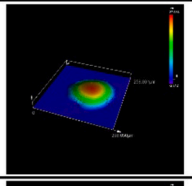	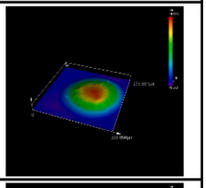
8. PLGA-75L-Gel					

Fig. 5. 3D scan images of 8 formulations in Table 1 in the dry state and after SSV exposure of each semi-solvent. Formulation 6 shows two batches (lot# 201111SMS and lot# 210608SMS) made at different times using the same manufacturing method.

Table 6
Selected parameters of each formulation. (Average ± standard deviation, $N = 10$, except Formulations 1 and 8 with $N = 9$).

Formulation 1	Sa	Sz	Ssk	Sku	Sal	Vmc	Sk	Hm	Rs
Dry	0.5 ± 0.2	15.0 ± 15.4	1.7 ± 5.2	67.8 ± 144.7	5.3 ± 1.4	0.4 ± 0.2	0.5 ± 0.2	117 ± 25	5.1 ± 0.25
Ethyl Isobutyrate	0.6 ± 0.4	12.2 ± 6.1	3.0 ± 0.8	17.1 ± 7.9	5.7 ± 1.5	0.5 ± 0.3	0.6 ± 0.2	118 ± 24	5.0 ± 0.2
Toluene	0.5 ± 0.4	9.3 ± 5.1	2.9 ± 1.3	17.0 ± 7.7	5.4 ± 1.6	0.4 ± 0.3	0.6 ± 0.3	118 ± 24	5.1 ± 0.3
2-Pentanone	0.3 ± 0.1	5.7 ± 2.0	2.6 ± 1.2	14.4 ± 3.6	5.8 ± 1.5	0.3 ± 0.1	0.5 ± 0.1	118 ± 26	4.5 ± 0.3
Propyl acetate	0.4 ± 0.1	7.2 ± 1.8	2.8 ± 1.6	16.1 ± 9.1	6.0 ± 1.3	0.3 ± 0.1	0.5 ± 0.2	101 ± 29	3.9 ± 0.7

Formulation 2	Sa	Sz	Ssk	Sku	Sal	Vmc	Sk	Hm	Rs
Dry	0.8 ± 0.6	23.6 ± 39.8	0.7 ± 6.4	43.8 ± 100.5	5.2 ± 1.2	0.56 ± 0.36	1.0 ± 1.1	103 ± 31	5.3 ± 0.5
Ethyl Isobutyrate	0.2 ± 0.1	2.1 ± 0.7	0.7 ± 1.7	9.8 ± 6.9	4.0 ± 1.0	0.13 ± 0.04	0.3 ± 0.1	100 ± 34	4.6 ± 0.5
Toluene	0.1 ± 0.0	2.3 ± 1.3	−0.5 ± 1.1	12.3 ± 6.5	6.8 ± 2.3	0.07 ± 0.03	0.11 ± 0.02	43 ± 17	1.4 ± 0.1
2-Pentanone	0.02 ± 0.01	1.0 ± 1.2	0.1 ± 2.3	49.6 ± 88.6	5.7 ± 2.5	0.02 ± 0.00	0.05 ± 0.01	25 ± 7	1.0 ± 0.0
Propyl acetate	0.03 ± 0.01	1.0 ± 0.8	−0.8 ± 1.7	25.9 ± 27.9	6.3 ± 2.7	0.02 ± 0.01	0.06 ± 0.02	22 ± 6	1.0 ± 0.0

Formulation 3	Sa	Sz	Ssk	Sku	Sal	Vmc	Sk	Hm	Rs
Dry	1.2 ± 2.2	17.1 ± 12.7	1.2 ± 2.9	31.3 ± 64.1	3.3 ± 1.7	0.7 ± 0.9	1.4 ± 2.8	75 ± 26	5.7 ± 0.9
Ethyl Isobutyrate	0.1 ± 0.1	6.0 ± 4.1	−0.8 ± 4.3	45.1 ± 59.3	4.6 ± 0.8	0.1 ± 0.1	0.1 ± 0.0	23 ± 10	1.2 ± 0.1
Toluene	0.1 ± 0.1	6.2 ± 5.4	−0.4 ± 3.3	29.5 ± 24.1	4.8 ± 0.9	0.1 ± 0.1	0.1 ± 0.0	23 ± 9	1.1 ± 0.1
2-Pentanone	0.1 ± 0.1	2.3 ± 2.4	−0.6 ± 2.1	21.6 ± 18.1	8.6 ± 4.1	0.1 ± 0.1	0.1 ± 0.1	13 ± 5	1.0 ± 0.0
Propyl acetate	0.1 ± 0.1	1.6 ± 1.8	0.2 ± 2.8	38.5 ± 43.8	10.6 ± 3.9	0.0 ± 0.1	0.1 ± 0.1	10 ± 5	1.0 ± 0.0

Formulation 4	Sa	Sz	Ssk	Sku	Sal	Vmc	Sk	Hm	Rs
Dry	0.7 ± 0.4	21.6 ± 21.1	−0.3 ± 2.8	54.4 ± 91.7	4.3 ± 0.8	0.5 ± 0.3	0.9 ± 0.3	99 ± 21	5.1 ± 0.3
Ethyl Isobutyrate	5.7 ± 1.4	56.9 ± 20.6	0.9 ± 0.6	5.2 ± 1.9	7.6 ± 1.2	5.9 ± 1.4	13.5 ± 5.8	90 ± 25	2.7 ± 1.2
Toluene	4.8 ± 2.7	51.1 ± 21.9	0.6 ± 0.5	5.0 ± 1.9	7.8 ± 1.6	4.9 ± 2.7	10.6 ± 8.6	87 ± 25	2.4 ± 1.3
2-Pentanone	2.2 ± 1.0	34.8 ± 12.3	0.1 ± 0.9	8.7 ± 5.6	6.9 ± 0.9	1.8 ± 1.1	3.1 ± 2.0	54 ± 13	1.5 ± 0.1
Propyl acetate	1.0 ± 0.4	23.3 ± 6.8	−0.2 ± 1.1	13.4 ± 3.6	5.9 ± 0.4	0.6 ± 0.2	1.3 ± 0.4	34 ± 9	1.2 ± 0.1

Formulation 5	Sa	Sz	Ssk	Sku	Sal	Vmc	Sk	Hm	Rs
Dry	4.2 ± 1.0	30.6 ± 11.5	1.0 ± 0.2	2.3 ± 0.7	6.1 ± 0.6	1.7 ± 0.7	4.3 ± 2.1	48 ± 13	5.1 ± 0.7
Ethyl Isobutyrate	0.9 ± 0.9	9.9 ± 6.9	0.1 ± 1.8	8.3 ± 7.0	3.7 ± 2.0	0.9 ± 0.9	2.1 ± 2.3	20 ± 7	2.3 ± 0.6
Toluene	0.8 ± 0.7	12.6 ± 6.3	0.0 ± 1.3	9.8 ± 7.8	5.3 ± 2.4	0.8 ± 0.7	2.0 ± 2.1	17 ± 6	1.8 ± 0.5
2-Pentanone	0.3 ± 0.5	6.6 ± 6.5	0.6 ± 1.6	18.6 ± 29.5	5.9 ± 1.3	0.3 ± 0.4	0.5 ± 0.7	10 ± 6	1.1 ± 0.3
Propyl acetate	0.2 ± 0.3	5.9 ± 5.6	1.6 ± 2.1	29.3 ± 44.1	6.0 ± 1.8	0.2 ± 0.2	0.3 ± 0.4	9 ± 5	1.1 ± 0.2

Formulation 6.1	Sa	Sz	Ssk	Sku	Sal	Vmc	Sk	Hm	Rs
Dry	3.6 ± 2.2	25.4 ± 11.9	0.9 ± 0.5	2.9 ± 1.1	5.5 ± 1.1	3.5 ± 3.4	6.2 ± 5.1	57 ± 20	5.5 ± 1.0
Ethyl Isobutyrate	1.0 ± 0.6	15.0 ± 6.7	−0.1 ± 0.3	5.6 ± 2.0	5.7 ± 1.6	1.0 ± 0.6	2.5 ± 1.4	26 ± 15	2.1 ± 0.7
Toluene	1.2 ± 0.6	18.1 ± 8.9	0.0 ± 0.4	4.8 ± 0.8	5.6 ± 1.9	1.2 ± 0.6	3.1 ± 1.6	27 ± 14	2.1 ± 0.7
2-Pentanone	1.4 ± 0.9	17.4 ± 9.8	0.3 ± 0.8	5.4 ± 2.2	6.0 ± 1.2	1.5 ± 1.0	3.6 ± 2.6	25 ± 15	1.8 ± 0.5
Propyl acetate	1.2 ± 0.8	16.0 ± 9.3	0.6 ± 1.0	6.0 ± 3.6	7.2 ± 1.8	1.2 ± 0.9	3.0 ± 2.3	25 ± 16	1.6 ± 0.5

Formulation 6.2	Sa	Sz	Ssk	Sku	Sal	Vmc	Sk	Hm	Rs
Dry	3.7 ± 0.6	26.3 ± 11.2	1.1 ± 0.2	1.9 ± 0.7	6.5 ± 0.4	1.4 ± 0.8	3.4 ± 1.8	49 ± 14	5.1 ± 0.3
Ethyl Isobutyrate	0.8 ± 0.4	15.6 ± 6.2	0.2 ± 0.8	10.8 ± 5.1	5.1 ± 1.0	0.6 ± 0.4	1.1 ± 0.8	18 ± 7	1.4 ± 0.2
Toluene	0.9 ± 0.4	16.5 ± 6.8	0.9 ± 1.7	13.3 ± 20.8	5.4 ± 1.4	0.7 ± 0.3	1.2 ± 0.6	19 ± 7	1.4 ± 0.2
2-Pentanone	0.9 ± 0.4	16.7 ± 6.0	1.1 ± 1.9	14.9 ± 28.3	5.1 ± 1.0	0.7 ± 0.3	0.9 ± 0.4	19 ± 7	1.4 ± 0.2
Propyl acetate	0.9 ± 0.4	17.0 ± 5.7	1.3 ± 2.2	17.1 ± 34.4	5.1 ± 1.0	0.6 ± 0.3	0.8 ± 0.3	18 ± 8	1.4 ± 0.2

Formulation 7	Sa	Sz	Ssk	Sku	Sal	Vmc	Sk	Hm	Rs
Dry	3.2 ± 0.3	40.2 ± 17.7	1.3 ± 0.3	4.6 ± 2.4	6.1 ± 0.5	2.0 ± 0.6	4.2 ± 1.1	69 ± 17	5.2 ± 0.3
Ethyl Isobutyrate	1.5 ± 0.9	16.7 ± 9.3	0.5 ± 1.9	9.1 ± 4.4	3.5 ± 1.2	1.1 ± 0.8	2.2 ± 1.6	65 ± 16	5.1 ± 0.6
Toluene	2.1 ± 2.3	19.6 ± 17.7	1.0 ± 1.5	6.9 ± 4.4	3.9 ± 2.0	2.1 ± 2.4	4.1 ± 4.7	61 ± 18	4.6 ± 1.1
2-Pentanone	0.2 ± 0.1	5.6 ± 4.4	−1.6 ± 1.5	16.4 ± 11.9	5.7 ± 1.1	0.2 ± 0.1	0.2 ± 0.1	17 ± 7	1.1 ± 0.1
Propyl acetate	0.1 ± 0.0	3.3 ± 2.0	1.1 ± 2.7	35.9 ± 38.1	6.1 ± 3.0	0.1 ± 0.0	0.1 ± 0.1	9 ± 4	1.0 ± 0.0

Formulation 8	Sa	Sz	Ssk	Sku	Sal	Vmc	Sk	Hm	Rs
Dry	3.4 ± 2.0	29.3 ± 16.8	0.5 ± 0.8	5.8 ± 5.2	3.4 ± 1.4	2.9 ± 2.1	6.8 ± 5.3	46 ± 24	5.3 ± 0.9

(*continued on next page*)

Table 6 (*continued*)

Formulation 8	Sa	Sz	Ssk	Sku	Sal	Vmc	Sk	Hm	Rs
Ethyl Isobutyrate	0.6 ± 0.4	12.9 ± 8.3	−0.3 ± 1.9	20.1 ± 15.0	3.0 ± 1.1	0.4 ± 0.2	0.8 ± 0.5	23 ± 22	2.2 ± 1.4
Toluene	0.1 ± 0.1	2.4 ± 1.4	2.0 ± 2.4	19.2 ± 20.7	6.6 ± 2.4	0.1 ± 0.1	0.2 ± 0.1	8 ± 6	1.0 ± 0.0
2-Pentanone	0.1 ± 0.0	2.6 ± 1.2	2.3 ± 2.4	26.3 ± 30.2	6.0 ± 1.5	0.1 ± 0.0	0.2 ± 0.1	7 ± 4	1.0 ± 0.0
Propyl acetate	0.1 ± 0.0	2.7 ± 1.3	2.5 ± 2.1	26.8 ± 29.1	6.1 ± 1.6	0.1 ± 0.0	0.2 ± 0.1	6 ± 3	1.0 ± 0.0

easily describe certain changes upon exposure to SSVs. This is the case if microparticles are made of PLGAs without drugs and other excipients. The presence of drugs and other excipients may complicate the structural changes of microparticles, requiring evaluation of other parameters. For Formulation 4, the 100 L portion of a polylithic particle collapsed, while the other 50 L parts remained intact during exposure to early semi-solvents. Significant changes occurred after exposure to 2-pentanone, as shown in Table 6. Although the 1:1 mixture of 50 L and 100 L resulted in the 'average' 75 L, Formulation 4 did not behave like Formulation 2. Formulation 4 displayed significantly higher Sa than Formulation 2 after exposure to ethyl isobutyrate, toluene, and 2-pentanone due to the inherent heterogeneity.

Differences in Formulations 5 and 6 are apparent in Fig. 5, but the image analysis in Table 6 provides a comprehensive understanding of the differences. The Sa value of Formulation 6 after exposure to 2-pentanone and propyl acetate was significantly higher than Formulation 5**. The Sa for Formulation 5 decreased substantially upon exposure to 2-pentanone, while Formulation 6 was less affected. The increased Sa in Formulation 6 was apparent visually (Fig. 5) by the more heterogeneous appearance of the particles, while Formulation 5 exhibits a smoother appearance. The same can be said for Sz, Vmc, Sk, Hm, and Rs. This means that Formulation 5 is more sensitive to 2-pentanone exposure than Formulation 6, which is shown by more pronounced shape changes by Formulation 5 upon exposure to 2-pentanone in Fig. 5. The surface of Formulation 6 became very heterogeneous, ranging from smooth peaks and wider valleys (as seen in Fig. 5) to sharper peaks and narrow valleys. Thus, examining many ROIs on diverse microparticles is more advantageous than a few images.

A comparison of Formulations 7 and 8 shows that significant changes in the parameters occurred after exposure to 2-pentanone and toluene for Formulations 7 and 8, respectively. For example, Sa, Sz, Sk, Hm, and Rs values of Formulation 7 dropped after exposure to 2-pentanone, while the same drop occurred after toluene exposure for Formulation 8. This is demonstrated by the significant differences in Sa*, Sal*, Sz**, Vvc**, Hm***, AR***, and several other parameters between Formulations 7 and 8 after toluene exposure. These differences decrease after 2-pentanone exposure due to further collapse of Formulation 7. The two formulations were prepared using the same PLGA and/or the same process; the only difference was the presence of leuprolide in Formulation 7. Thus, it is expected that the presence of leuprolide affected the microstructures to alter the PLGA dissolution properties in semi-solvents.

Reproducibility of the method was evaluated utilizing repeat testing of Formulation 6 using a secondary batch manufactured by the same method as the original. In the morphological examination, the results of both tests were reproducible, as shown in Fig. 5. Microparticles from both batches showed the same general trend of collapsing rapidly upon exposure to ethyl isobutyrate to a porous, molten structure. By the numbers, trends between microparticles from each batch were consistent. Although there were occasional differences in the exact values for the particles at occasional points due to random sampling, the trends were consistent in demonstrating decreases in height parameters (Sa, Sz, Hm Rs, Sk, etc.) as a result of the collapse of the particle under solvent effects yet still maintained higher roughness (using Sa as an indicator) than blank particles in Formulation 2 towards the later solvents such as 2-pentanone and propyl acetate which exhibited <0.1 μm Sa due to highly smooth surface. This replicate testing with separately manufactured batches exhibits method validation for reproducibility; however, it also highlights that the best way to obtain optimal data for the detection of manufacturing differences within this method is to utilize a series of tests with high particle numbers (high N) to average out the variance introduced simply by random sampling.

There are dozens of parameters that can characterize the surface roughness. The goal was to find parameters that could quantitatively explain changes in visual images. In this study, nine parameters were chosen to describe the morphological changes in visual images. The rest of the vast data produced by LEXT, a laser scanning confocal microscope, is available for analysis of different aspects of microparticles, future use, or use by other investigators. The selection of image analysis parameters may likely change depending on the goal of the analysis. Thus, the method will require customization to the formulation in question. Overall, SASSI-SSV provides a means to detect differences in the microstructures of PLGA formulations, which are not readily detectable by DSC or polymer characterization.

4. Discussion

Long-acting injectable (LAI) formulations deliver a variety of drugs ranging from small hydrophobic drugs to peptide drugs for up to 6 months. Such a long-acting property was obtained from different PLGA polymers in the microparticles, in-situ forming gels, and implant forms. Controlling the drug release kinetics is of prime importance in providing safe and effective amounts of drugs to patients [28,29]. When LAI systems are prepared to make new formulations or generic versions of brand name products, their thorough characterization is critical to ensure that the formulations function as intended. Conforming the drug release properties for LAI formulations that deliver drugs for months is not trivial. Thus, it is necessary to find methods to characterize PLGA polymers and their formulations. Numerous research articles have provided information on PLGA-based LAI formulations, such as the impact of formulation, manufacturing, and experimental variables on drug release kinetics, to understand better the drug release mechanisms [8,11–13,26,30–51].

In-depth characterization of PLGA polymers has helped evaluate and compare formulations with different compositions and/or manufacturing processes. As a result, significant advances have been achieved recently in developing assays to establish the match of qualitative (same type) and quantitative (same amount) properties of a proposed generic to the respective reference listed drug product [51,52]. Another question that needs to be answered is whether different PLGA formulations can be identified based on their 3D structural arrangement. Typically, microparticle formulations are created by emulsion methods. Even minor changes in PLGA type, solvent, pH, temperature, agitation rate, and other processing parameters drastically affect the microparticle structure and resultant drug release kinetics [37,52]. In addition to the material properties of the PLGA type and drug content, the drug release rate can be significantly affected by the microstructure of the manufactured PLGA microparticles. This includes the distribution of the drug across the microparticle (interior versus surface, evenly dispersed or present as discrete crystals or in amorphous form), presence of other excipient components, residual solvents, interactions between drug and polymer, as well as a plethora of other factors which could affect the drug release and degradation properties of the microparticles.

Although the qualitative properties of PLGA in microparticles can be obtained by extraction and analysis, as well as the morphological properties by conventional imaging techniques, there remains a lack to

bridge these two properties. There is a need for advanced analytical methods and tools to comprehensively understand microparticles' microstructure and behavior. The polymer composition, arrangement, and interaction with drug molecules can be studied by carefully controlling the access of particles to vapor-phase semi-solvents and monitoring the resultant changes in morphological behavior. Conventionally, the ability of PLGA polymers and microparticles to absorb solvent vapors has not been exploited in controlled drug delivery applications, while it has been in industrial manufacturing of solar cells, sensors, and other oriented polymer structures [53]. However, alternative methods were tested due to the excessive solvating power of the liquid solvents and the non-trivial difficulty of handling the liquid solvents. The exposure of PLGA microparticles to semi-solvents in their vapor phase solved many practical limitations associated with liquid solvent exposure, such as the variability introduced by the liquid solvent handling procedure, rapid microparticle collapse, and dissolution resulting from their highly efficient solvation ability.

For the current test of reviewing morphological changes, the impact of the semi-solvent can be more accurately described as plasticization, which can occur under conditions that are not as aggressive as dissolution. Small quantities of vapor can plasticize and melt the PLGA, while larger quantities of solvent as a liquid would be necessary to dissolve fully). Despite this, the relative impact of solubilization relative to a semi-solvent's ability to affect PLGA at a specific L:G ratio plays a vital role in the particle behavior under the plasticization effect. This can be observed by the differences between Formulations 1 (PLGA-50 L), 2 (PLGA-75 L), and 3 (PLA-100 L). Formulation 1 is more highly resistant to changes due to semi-solvent exposure than Formulation 2. Additionally, Formulation 3 exhibits quick plasticization and melting behavior even with semi-solvent vapors that require high lactide content to operate. This indicates that the polymer-solvent plasticization behavior agrees with the polymer-solvent dissolution behavior.

One limitation of surface scanning confocal microscopy is that the reflected pixel from the highest z-scan is collected as the surface data point [54]. This is unlike fluorescence confocal microscopy, which relies on the light generated by fluorophores within the 3D space of the imaging field. Due to this limitation, features at extreme slopes or along the underside of a surface (i.e., covered by the shadow of a feature at a higher z-focal plane above that location) cannot be imaged. In this regard, surface scanning confocal microscopy provides a similar type of information as atomic force microscopy (AFM), which does not provide information regarding the sides or bottom [55]. Unlike AFM, however, surface scanning microscopy can provide information for larger areas or multiple samples to quickly obtain robust averaging of data. Due to this limitation, only the top surface of spherical particles can be imaged, while the sides and bottom of the particles are not included as collected information. Despite this limitation, this technique can provide critical information regarding the surface conditions of the particles. One of the contributing factors to the measured values is the measurable area of the microparticles. For calculations, a ROI is established across the measurable parts of the particles for profilometry analysis. As the confocal laser imaging provides a top-down view of the particles, no scan data is obtained regarding the sides and bottom of the spherical particle as these portions are shadowed by the top of the particle. This can vary the measured results based on how much of the particle is observable and the total depth available (distance from the top of the melted particle to the glass surface) for features to present themselves.

The microparticle morphological behavior under exposure to semi-solvents provides insights into the microstructural orientation and composition of the particles. The exact interpretation of this morphological behavior depends on the active pharmaceutical ingredient and formulation properties. The particle morphological comparison in this study is designed to compare different sets of microparticles to examine whether they are made of the same formulation compositions or by the same process or not. It is too early to tell whether the microparticle morphology is related to the drug release properties. While it is expected to be true, more extensive studies are necessary to establish such a correlation.

Sometimes the observed visual difference does not appear to match the quantitative values of image analysis. This is mainly because the average values obtained by the image analysis are for all microparticles examined. The images shown in Fig. 5 are only representative images of different formulations. Thus, one image in Fig. 5 may not be the same as all other images of the formulation. Each microparticle is different, and the measured parameters reflect the individuality of the microparticles and measurements across a diverse set of microparticles, all of which are unique. Thus, the image analysis parameters may appear off from the visual observation. However, if the data in Table 6 are studied carefully, they represent the overall changes of all microparticles after exposure to semi-solvents. Sometimes, the standard deviation is massive, e.g., the Sku value of Formulation 5 changed from 9.8 ± 7.8 to 18.6 ± 29.5 after 2-pentanone treatment, indicating the dramatic transformation of the surface morphology on some microparticles. All microparticles of each test sample will follow the same transformation if given more time or exposed to SSV longer. A simple solution to overcome this issue is to increase the number of microparticles tested.

CRediT authorship contribution statement

John Garner: Conceptualization, Methodology, Investigation, Validation, Formal analysis, Resources, Data curation, Writing – original draft, Visualization. **Sarah Skidmore:** Methodology, Investigation, Validation, Resources, Writing – original draft. **Justin Hadar:** Methodology, Investigation, Validation, Resources, Writing – original draft. **Haesun Park:** Conceptualization, Formal analysis, Writing – review & editing, Supervision, Project administration, Funding acquisition. **Kinam Park:** Conceptualization, Writing – review & editing, Supervision. **Bin Qin:** Conceptualization, Formal analysis, Writing – review & editing, Project administration. **Yan Wang:** Conceptualization, Formal analysis, Writing – review & editing, Project administration.

Acknowledgments

This work was supported by BAA Contract # 75F40119C10096 from the Center for Drug Evaluation Research of the Food and Drug Administration (FDA) and in part by the Ralph W. and Grace M. Showalter Research Trust Fund. The contents are solely the authors' responsibility and do not necessarily represent the official views of the FDA.

References

[1] J. Garner, S. Skidmore, H. Park, K. Park, S. Choi, Y. Wang, A protocol for assay of poly (lactide-co-glycolide) in clinical products, Int. J. Pharm. 495 (2015) 87–92.
[2] J. Garner, S. Skidmore, H. Park, K. Park, S. Choi, Y. Wang, Beyond Q1/Q2: the impact of manufacturing conditions and test methods on drug release from PLGA-based microparticle depot formulations, J. Pharm. Sci. 107 (2018) 353–361.
[3] K. Park, S. Skidmore, J. Hadar, J. Garner, H. Park, A. Otte, B.K. Soh, G. Yoon, D. Yu, Y. Yun, B.K. Lee, X.J. Jiang, Y. Wang, Injectable, long-acting PLGA formulations: analyzing PLGA and understanding microparticle formation, J. Control. Release 304 (2019) 125–134.
[4] S. Skidmore, J. Hadar, J. Garner, H. Park, K. Park, Y. Wang, X.J. Jiang, Complex sameness: separation of mixed poly(lactide-co-glycolide)s based on the lactide: glycolide ratio, J. Control. Release 300 (2019) 174–184.
[5] J. Hadar, S. Skidmore, J. Garner, H. Park, K. Park, Y. Wang, B. Qin, X. Jiang, D. Kozak, Method matters: development of characterization techniques for branched and glucose-poly(lactide-co-glycolide) polymers, J. Control. Release 320 (2020) 484–494.
[6] J. Garner, S. Skidmore, J. Hadar, H. Park, K. Park, Y. Kuk Jhon, B. Qin, Y. Wang, Analysis of semi-solvent effects for PLGA polymers, Int. J. Pharm. 602 (2021), 120627 (120627 pages).
[7] K. Park, A. Otte, F. Sharifi, J. Garner, S. Skidmore, H. Park, Y.K. Jhon, B. Qin, Y. Wang, Formulation composition, manufacturing process, and characterization of poly(lactide-co-glycolide) microparticles, J. Control. Release 329 (2021) 1150–1161.
[8] J.V. Andhariya, S. Choi, Y. Wang, Y. Zou, D.J. Burgess, J. Shen, Accelerated in vitro release testing method for naltrexone loaded PLGA microspheres, Int. J. Pharm. 520 (2017) 79–85.

[9] J.V. Andhariya, J. Shen, S. Choi, Y. Wang, Y. Zou, D.J. Burgess, Development of in vitro-in vivo correlation of parenteral naltrexone loaded polymeric microspheres, J. Control. Release 255 (2017) 27–35.

[10] F. Sharifi, A. Otte, G. Yoon, K. Park, Continuous in-line homogenization process for scale-up production of naltrexone-loaded PLGA microparticles, J. Control. Release 325 (2020) 347–358.

[11] K. Hirota, A.C. Doty, R. Ackermann, J. Zhou, K.F. Olsen, M.R. Feng, Y. Wang, S. Choi, W. Qu, A.S. Schwendeman, S.P. Schwendeman, Characterizing release mechanisms of leuprolide acetate-loaded PLGA microspheres for IVIVC development I: in vitro evaluation, J. Control. Release 244 (2016) 302–313.

[12] J. Zhou, K. Hirota, R. Ackermann, J. Walker, Y. Wang, S. Choi, A. Schwendeman, S. P. Schwendeman, Reverse engineering the 1-month Lupron depot®, AAPS J. 20 (2018) 105 (113 pages).

[13] J. Liang, Y. Wang, B. Qin, J. Zhou, S. Schwendeman, J. Zheng, Micro-imaging and microanalysis of PLGA complex drug products by scanning electron microscopy (SEM), Microsc. Microanal. 26 (2020) 2266–2268.

[14] J. Zhou, J. Walker, R. Ackermann, K. Olsen, J.K. Hong, Y. Wang, S. P. Schwendeman, Effect of manufacturing variables and raw materials on the composition-equivalent PLGA microspheres for 1-month controlled release of leuprolide, Mol. Pharm. 17 (2020) 1502–1515.

[15] PINMRF, Purdue Interdepartmental NMR Facility. https://www.pinmrf.purdue.edu/services/.

[16] S. Van der Jeught, J.J. Dirckx, Real-time structured light profilometry: a review, Opt. Lasers Eng. 87 (2016) 18–31.

[17] GraphPad, t test Calculator. https://www.graphpad.com/quickcalcs/ttest1/?format=SD, 2022.

[18] F. Blateyron, Filtration Techniques for Surface Texture. https://guide.digitalsurf.com/en/guide-filtration-techniques.html, 2021.

[19] Q. Qi, T. Li, P.J. Scott, X. Jiang, A correlational study of areal surface texture parameters on some typical machined surfaces, Proc. CIRP 27 (2015) 149–154.

[20] Keyence, Introduction to Surface Roughness Measurement. https://sernia.ru/upload/pdf_files/Introduction%20to%20surface%20roughness%20measurement.pdf, 2012.

[21] Keyence, Compare and Understand. Selecting Roughness Measuring Instrument, 2020.

[22] C.E. Rapier, K.J. Shea, A.P. Lee, Investigating PLGA microparticle swelling behavior reveals an interplay of expansive intermolecular forces, Sci. Rep. 11 (2021) 1–12.

[23] A. Dobhal, A. Srivastav, P. Dandekar, R. Jain, Influence of lactide vs glycolide composition of poly (lactic-co-glycolic acid) polymers on encapsulation of hydrophobic molecules: molecular dynamics and formulation studies, J. Mater. Sci. Mater. Med. 32 (2021) 126 (118 pages).

[24] S.G. Wright, M.E. Rickey, J.M. Ramstack, S.L. Lyons, J.M. Hotz, Method for preparing microparticles having a selected polymer molecular weight (2003) US 6,534,092.

[25] S. D'Souza, J.A. Faraj, R. Dorati, P.P. DeLuca, Enhanced degradation of lactide-co-glycolide polymer with basic nucleophilic drugs, Adv. Pharm. 2015 (2015), 10 pages.

[26] M. Kohno, J.V. Andhariya, B. Wan, Q. Bao, S. Rothstein, M. Hezel, Y. Wang, D. J. Burgess, The effect of PLGA molecular weight differences on risperidone release from microspheres, Int. J. Pharm. 582 (2020), 119339.

[27] X. Luan, R. Bodmeier, Influence of the poly (lactide-co-glycolide) type on the leuprolide release from in situ forming microparticle systems, J. Control. Release 110 (2006) 266–272.

[28] W.Y. Lee, M. Asadujjaman, J.-P. Jee, Long acting injectable formulations: the state of the arts and challenges of poly (lactic-co-glycolic acid) microsphere, hydrogel, organogel and liquid crystal, J. Pharm. Investig. 49 (2019) 459–476.

[29] C.I. Nkanga, A. Fisch, M. Rad-Malekshahi, M.D. Romic, B. Kittel, T. Ullrich, J. Wang, R.W.M. Krause, S. Adler, T. Lammers, W.E. Hennink, F. Ramazani, Clinically established biodegradable long acting injectables: an industry perspective, Adv. Drug Deliv. Rev. 167 (2020) 19–46.

[30] K.G.H. Desai, S.R. Mallery, S.P. Schwendeman, Effect of formulation parameters on 2-methoxyestradiol release from injectable cylindrical poly (DL-lactide-co-glycolide) implants, Eur. J. Pharm. Biopharm. 70 (2008) 187–198.

[31] A.C. Doty, D.G. Weinstein, K. Hirota, K.F. Olsen, R. Ackermann, Y. Wang, S. Choi, S.P. Schwendeman, Mechanisms of in vivo release of triamcinolone acetonide from PLGA microspheres, J. Control. Release 256 (2017) 19–25.

[32] M. Yu, W. Yuan, D. Li, A. Schwendeman, S.P. Schwendeman, Predicting drug release kinetics from nanocarriers inside dialysis bags, J. Control. Release 315 (2019) 23–30.

[33] A. Rawat, D.J. Burgess, Effect of ethanol as a processing co-solvent on the PLGA microsphere characteristics, Int. J. Pharm. 394 (2010) 99–105.

[34] A. Rawat, D.J. Burgess, Effect of physical ageing on the performance of dexamethasone loaded PLGA microspheres, Int. J. Pharm. 415 (2011) 164–168.

[35] J.V. Andhariya, D.J. Burgess, Recent advances in testing of microsphere drug delivery systems, Expert Opin. Drug Deliv. 13 (2016) 593–608.

[36] J.V. Andhariya, J. Shen, Y. Wang, S. Choi, D.J. Burgess, Effect of minor manufacturing changes on stability of compositionally equivalent PLGA microspheres, Int. J. Pharm. 566 (2019) 532–540.

[37] Q. Bao, Y. Zou, Y. Wang, S. Choi, D.J. Burgess, Impact of formulation parameters on in vitro release from long-acting injectable suspensions, AAPS J. 23 (2021) 1–11.

[38] N. Faisant, J. Siepmann, J.P. Benoit, PLGA-based microparticles: elucidation of mechanisms and a new, simple mathematical model quantifying drug release, Eur. J. Pharm. Sci. 15 (2002) 355–366.

[39] N. Faisant, J. Akiki, F. Siepmann, J.P. Benoit, J. Siepmann, Effects of the type of release medium on drug release from PLGA-based microparticles: experiment and theory, Int. J. Pharm. 314 (2006) 189–197.

[40] D. Klose, F. Siepmann, K. Elkharraz, J. Siepmann, PLGA-based drug delivery systems: importance of the type of drug and device geometry, Int. J. Pharm. 354 (2008) 95–103.

[41] D. Klose, C. Delplace, J. Siepmann, Unintended potential impact of perfect sink conditions on PLGA degradation in microparticles, Int. J. Pharm. 404 (2011) 75–82.

[42] H. Gasmi, F. Danede, J. Siepmann, F. Siepmann, Does PLGA microparticle swelling control drug release? New insight based on single particle swelling studies, J. Control. Release 213 (2015) 120–127.

[43] H. Gasmi, F. Siepmann, M.C. Hamoudi, F. Danede, J. Verin, J.F. Willart, J. Siepmann, Towards a better understanding of the different release phases from PLGA microparticles: dexamethasone-loaded systems, Int. J. Pharm. 514 (2016) 189–199.

[44] M.C. Hamoudi-Ben Yelles, V. Tran Tan, F. Danede, J.F. Willart, J. Siepmann, PLGA implants: how Poloxamer/PEO addition slows down or accelerates polymer degradation and drug release, J. Control. Release 253 (2017) 19–29.

[45] F. Tamani, C. Bassand, M.C. Hamoudi, F. Danede, J.F. Willart, F. Siepmann, J. Siepmann, Mechanistic explanation of the (up to) 3 release phases of PLGA microparticles: Diprophylline dispersions, Int. J. Pharm. 572 (2019), 118819.

[46] J. Siepmann, F. Siepmann, Sink conditions do not guarantee the absence of saturation effects, Int. J. Pharm. 577 (2020), 119009.

[47] F. Tamani, M.C. Hamoudi, F. Danede, J.-F. Willart, F. Siepmann, J. Siepmann, Towards a better understanding of the release mechanisms of caffeine from PLGA microparticles, J. Appl. Polym. Sci. 137 (2020), 48710 (48712 pages).

[48] K. Vay, S. Scheler, W. Frieß, New insights into the pore structure of poly(D,L-lactide-co-glycolide) microspheres, Int. J. Pharm. 402 (2010) 20–26.

[49] K. Vay, S. Scheler, W. Frieß, Application of Hansen solubility parameters for understanding and prediction of drug distribution in microspheres, Int. J. Pharm. 416 (2011) 202–209.

[50] K. Vay, Analysis and control of the manufacturing process and the release properties of PLGA microparticles for sustained delivery of a poorly water-soluble drug. https://edoc.ub.uni-muenchen.de/15049/1/Vay_Kerstin.pdf, 2012.

[51] K. Vay, W. Frieß, S. Scheler, A detailed view of microparticle formation by in-process monitoring of the glass transition temperature, Eur. J. Pharm. Biopharm. 81 (2012) 399–408.

[52] Y. Ma, J. Liang, J. Zheng, Y. Wang, M. Ashraf, C. Srinivasan, Significance of cryogenic broad ion beam milling in evaluating microstructures of PLGA-based drug products, Microsc. Microanal. 27 (2021) 90–91.

[53] H. Tang, G. Lu, L. Li, J. Li, Y. Wang, X. Yang, Precise construction of PCBM aggregates for polymer solar cells via multi-step controlled solvent vapor annealing, J. Mater. Chem. 20 (2010) 683–688.

[54] M. Farell, Principles of laser scanning microscopes. Part II: resolving power, measurement accuracy, software for laser scanning microscopes, and an application note, PhotonicsViews 18 (2021) 100–104.

[55] D. Khanal, B. Zhang, I. Ramzan, C. Marcott, Q. Li, W. Chrzanowski, Probing chemical and mechanical nanodomains in copolymer nanorods with correlative atomic force microscopy—nano-correscopy, Part. Part. Syst. Charact. 35 (2018) 1700409.